Materials and Design 84 (2015) 245–253

Contents lists available at ScienceDirect

Materials and Design

journal homepage: www.elsevier.com/locate/jmad

The role of oxidation and counterface in the high temperature tribological properties of TiAl intermetallics

Jun Cheng, Fei Li, Zhuhui Qiao *, Shengyu Zhu, Jun Yang *, Weimin Liu

State Key Laboratory of Solid Lubrication, Lanzhou Institute of Chemical Physics, Chinese Academy of Sciences, Lanzhou 730000, PR China

ARTICLE INFO

Article history:
Received 26 February 2015
Received in revised form 1 June 2015
Accepted 20 June 2015
Available online 28 June 2015

Keywords:
Intermetallics
Titanium aluminides
High temperature
Tribological properties
Counterface materials
Oxidation behavior

ABSTRACT

Clarification of how oxidation and counterface materials influence the high temperature tribological properties of TiAl alloy is the main object of this research. As evident from the comparison tests in air and argon, surface oxidation is detrimental to the tribological properties of the alloy at low temperature, but favorable above 600 °C. Counterface (Si_3N_4, SiC and Al_2O_3) is an important factor that largely affects the tribological properties of TiAl alloys, and this effect is strongly dependent on the system environment. In general, TiAl alloy shows superior tribological properties when Al_2O_3 is mating surface, excluding at 800 °C in argon.

1. Introduction

Because of the excellent properties of high strength-to-density ratio, oxidation resistance and high temperature strength, TiAl-based alloy has been considered as a new generation of lightweight high-temperature structural materials for aerospace and automotive applications including turbine blades, divergent flap, turbocharger wheels, nozzles and exhaust valves [1–4]. However, considerable works, involving the improvement of room temperature ductility and better understanding of tribological behaviors, should be carried out to realize the engineering application of the TiAl alloys. Despite the fact that the research on the tribological properties of the TiAl alloy has received substantial interest [5–12], a systematic study about the effect of the oxidation on the tribological properties of the TiAl alloy is lacking, especially at the elevated temperature. It has been reported that the formation of oxides during wear process in an oxidizing environment is likely to reduce wear of materials by preventing severe direct contact between the tribo-pairs or forming a protective oxide glaze [13–17]. But there has been controversy because some references have noted that the surface oxidation is not always functional in reducing wear, depending on the types, chemistry and structure of oxides [13]. With specific focus on TiAl alloys, room temperature pin-on-disk tribotests on a Ti–47Al–2Cr–2Nb–0.2 W alloy have shown that this type of alloy is sensitive to the presence of oxygen, i.e. it has much lower wear rates in the oxygen-free environments [18]. Similar results were found by Cheng et al. [10]: the wear rate of the Ti–46Al–2Cr–2Nb alloy in high vacuum is almost an order of magnitude lower than that in air. In our previous paper, the high-temperature tribological behaviors of the TiAl alloy in air were investigated and revealed that there is a wear mechanism transition due to the occurrence of brittle-to-ductile transition of TiAl alloy [19]. Whereas how oxidation influences the tribological behaviors at a wide temperature range is not well evaluated and understood. Clarification of this issue would be vital to the high temperature applications of TiAl alloys and helpful to design the self-lubricity and wear-resistance in TiAl-based composites.

Second, the wear and friction behavior is not an inherent property of material, but is a system-response that not only depends on the composition, property of the materials but also depends on the testing parameters including counterface selection [20,21]. It is noted that under dry-sliding condition, wear loss of TiAl in the contact pair of TiAl/Al_2O_3 is the highest, and that in the pair of TiAl/steel is the lowest [20]. Xu et al. [21] also observed that the room-temperature tribological properties of TiAl alloy are strongly dependent on the counterface materials. But whether or not such dependency will change once taking into account the oxygen-free environment and high temperature that simulates the potential service conditions of titanium aluminides, is not studied.

In this paper, tribological properties of a TiAl alloy against Si_3N_4, Al_2O_3 and SiC balls in air and argon from room temperature to 800 °C were compared, aiming at the above two questions.

2. Experimental procedures

A Ti–46Al–2Cr–2Nb (atomic ratio) alloy was selected as the experimental material. The starting materials were Ti (99% purity, <48 μm),

* Corresponding authors.
E-mail addresses: zhqiao@licp.cas.cn (Z. Qiao), jyang@licp.cas.cn (J. Yang).

http://dx.doi.org/10.1016/j.matdes.2015.06.115
0264-1275/

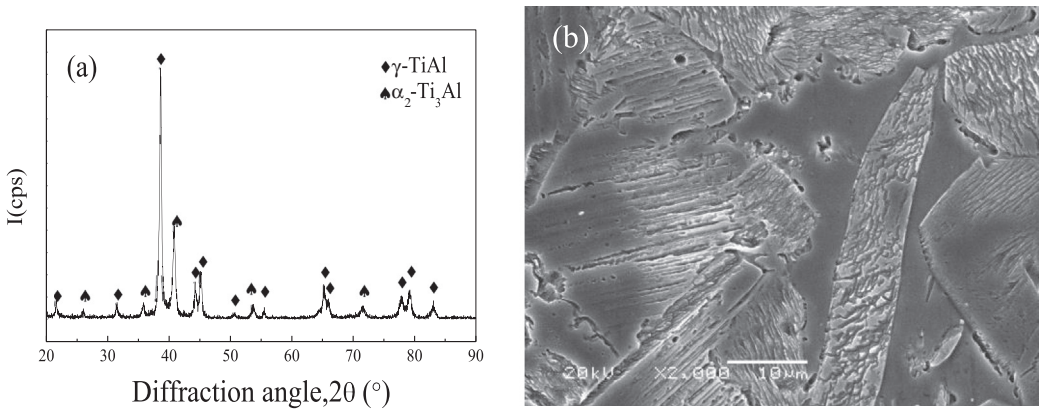

Fig. 1. The XRD pattern (a) and SEM image (b) of the Ti–46Al–2Cr–2Nb alloy [19].

Al (99% purity, <150 μm), Cr (99% purity, <75 μm), and Nb (99% purity, <150 μm). Before sintering, the mixed powders of Ti, Al, Cr and Nb with an atomic ratio of 50:46:2:2 were dry milled uniformly under argon atmosphere for 8 h. Then, the mixed powder was enclosed into BN-coated graphite mold and sintered at the temperature of 1350 °C and the pressure of 30 MPa holding 30 min, protected by high purity argon atmosphere. The sintered products were about 50 mm in diameter and 20 mm in thick. As follows, the sintered samples were machined to desired sizes for different tests. Prior to the tests, the machined samples were ground with a 1000-grit emery paper, and then metallographically polished.

The phase composition and microstructure of the alloy were identified by X-ray diffraction (XRD) and scanning electron microscope (SEM). The density was measured by Archimedes' principle. A universal material testing machine was employed to measure the three-point bending and compression strength of the material. The results [19], as shown in Fig. 1 and Table. 1, indicate that the alloy mainly consists of γ-TiAl phase and a small amount of α_2-Ti_3Al phase, and the microstructure is a duplex structure. The density and strength of the Ti–46Al–2Cr–2Nb alloy is comparable to a cast Ti–41.7Al–8.3Nb–0.09Y alloy.

The friction and wear tests were performed on a home-built ball-on-disk test rig. Fig. 2 shows the schematic picture of this tribometer. The alloy disk with a dimension of 19 × 19 × 4 mm^3 was rotated against a stationary ball of 6 mm diameter.

The counterface sliders were commercial balls of Si_3N_4, Al_2O_3 and SiC (Jienaier Cemented Carbides co., LTD) and Table 2 lists their properties obtained from manufacturers' data. The error ranges of these properties are controlled within ± 10%. The experimental parameters were: applied load = 10 N, testing time = 30 min, sliding speed = 0.188 m s^{-1} and wear track diameter = 10 mm. The selected temperatures were 20, 200, 400, 600 and 800 °C. The tests were carried out in air and argon with a continuous flow of 5 L/min. It is noted that the oxygen content in the Ar is 2 PPM, thus it is speculated that the oxygen partial pressure is in the order of 10^{-6} atm during wear test. The friction force was obtained by the detector of tribometer. Then, the friction coefficient was evaluated automatically by the software of the instrument in term of the equation: μ = F/Q (F is the friction force and Q is the normal load). In general, a tribo-pairs exhibits an initial running period in which the friction coefficient is unstable and the time is no more than several minutes. At the end of this period, the friction coefficient achieves a stable value, which was reported. After the tribological tests, the morphologies of the worn surfaces were examined by SEM (JSM-5600LV) equipped with energy dispersive spectroscopy (EDS). A contact surface profilometer (Model 2206, Harbin Measuring and cutting Tool Group Co., Ltd) was used to measure the cross-sections of the worn surface and wear volume was calculated using the integral method. The wear rate was calculated as wear volume divided by sliding distance and applied load. A non-contact surface profilometer (Micro-XAM-3D) was employed to generate high-resolution 3D images and cross-section profiles of the wear scar of the alloy by white light interferometry. All the tribological tests and measurements were carried out at least three times under identical conditions to make sure of the reliability of the data.

3. Results

3.1. Friction and wear properties of the TiAl alloy

Fig. 3 shows the friction coefficient of the alloy against Si_3N_4, Al_2O_3 and SiC balls at different temperatures in air and argon respectively. As shown, whatever the counterface materials, the friction coefficient of the alloy in argon is lower or at least comparable to that in air.

For the effect of the counterface on the friction behavior of TiAl alloy, it is seen that in air, the friction coefficient of the alloy against Al_2O_3 and SiC at 20 and 200 °C is considerably lower than that against Si_3N_4, while TiAl/SiC tribopair exhibits the highest friction coefficient at 400 to 800 °C. In argon, 600 °C is a transition point, below which the friction coefficient of the alloy is insensitive to the counterface materials, but above this point, the friction coefficient becomes sensitive to the counterface materials, according to the following ranking: $TiAl/Al_2O_3 < TiAl/SiC < TiAl/Si_3N_4$.

Fig. 4 shows the wear rate of the alloy against Si_3N_4, Al_2O_3 and SiC balls at different temperatures in air and argon respectively. In short, at the temperature from 20 to 600 °C the wear rate of the alloy in air is markedly higher than those in argon. When the temperature is up to 800 °C, the alloy is worn much more in argon than in air, especially coupled with Al_2O_3.

In addition, the effect of the counterface materials on the wear rate of TiAl alloy is strongly correlated to the system environment. The wear rate of the alloy in air below 400 °C is sensitive to the counterface

Table 1
Characteristics of the Ti–46Al–2Cr–2Nb and Ti–41.7Al–8.3Nb–0.09Y alloys studied [19].

Materials	Hardness (GPa)	Bending strength (MPa)	Compressive strength (MPa)	Density (g/cm^3)
Ti–46Al–2Cr–2Nb	3.65	563	1512	4.02
Ti–41.7Al–8.3Nb–0.09Y	3.85	565	1916	4.32

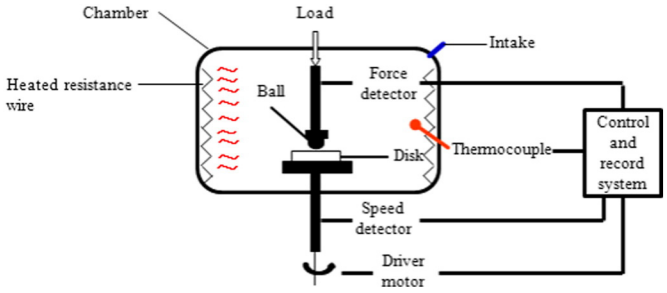

Fig. 2. The schematic picture of the tribometer.

Table 2
Characteristics of the counterface balls used in this study.

Materials	Hardness (GPa)	Compressive strength (MPa)	K_{IC} (MPa $m^{1/2}$)
Al_2O_3	16.5	2200	4.2
Si_3N_4	15	1800	6.2
SiC	28	2300	3.9

materials, i.e. TiAl sliding against Al_2O_3 produces the lowest wear rate, followed by TiAl/SiC and TiAl/Si_3N_4 tribopairs. However, counterface influence on the wear rate of the alloy is negligible in air above 600 °C. In argon the difference in the wear rate caused by counterface is moderate but pronounced at 800 °C. It is seen that at the temperature from 20 to 600 °C in argon, testing the alloy against Al_2O_3 also results in lower wear rate and the wear rates of the alloy mated with SiC and Si_3N_4 are analogous. But at 800 °C in argon, the highest wear rate is obtained for the alloy against Al_2O_3.

3.2. Surface analyses of the TiAl alloy and counterface materials in air and argon

Fig. 5 shows the morphologies of the worn surfaces of the alloy and counterface balls at different temperatures in argon. It is clear that under all the testing temperatures in argon, there are some grooves on all the worn surfaces of TiAl alloy against the three counterface balls, indicating that the wear mechanism of TiAl alloy in argon is dominated by abrasion wear. Further examination shows that the worn surfaces of the TiAl alloys differ depending on the counterpart material, indicating a slight change of wear mechanism. For sliding contact of TiAl/Si_3N_4, the increase of the temperature from 20 to 600 °C accelerates the abrasion wear, demonstrated by much more numerous and deeper grooves. But for TiAl/Al_2O_3 and TiAl/SiC tribo-pairs, the worn surfaces of the alloy are fairly smooth along with shallow grooves at temperature range 20 to 600 °C. At 800 °C, the worn surface of TiAl alloy is rougher and the quantity of fine particles is higher when the mating surfaces are Al_2O_3 and SiC than when the mating surface is Si_3N_4, sourced from relatively severe abrasion wear.

Apart from the abrasion wear, SEM observation on the worn surfaces of counterface balls (inserted in Fig. 5) provides the clear evidence for the transfer of the alloy and thus, slight adhesion wear occurs. With the aid of surface chemical composition analyses by EDS (Table. 3), the quantity of transfer materials on the Al_2O_3 ball below 600 °C in argon is considerably lower than those on SiC and Si_3N_4 balls. On the contrary, the Al_2O_3 surface at 800 °C is covered by abundant transfer materials while SiC and Si_3N_4 surfaces are pretty clear. This discrepancy on the transfer of TiAl alloy depending on counterface materials seems to be responsible for the slight wear difference of TiAl alloy in argon.

Fig. 6 shows the 3D images and cross-section profiles of the worn surfaces of the alloy against different balls at different temperatures in argon. In general, the wear scar of the alloy generated by SiC ball is much wider than that when the alloy runs against Si_3N_4 and Al_2O_3, which is consistent with the larger worn cap of SiC ball in Fig. 5. This is possibly attributed to the low fracture toughness of SiC ball that may be easily fractured by external stress during wear tests. From the analyses of the cross-section profiles, it is found that with the Al_2O_3 as the mating surface, the depth and width of the wear scar of the alloy is nearly the lowest between room temperature and 600 °C, corresponding to the highest wear resistance. While at 800 °C the wear scar widths of the alloy sliding against the three counterface materials are nearly the same, but the alloy coupled with Al_2O_3 experiences the maximum depth and thus has a high wear.

Fig. 7 shows the morphologies of the worn surfaces of the alloy and counterface balls at different temperatures in air. In air, deep grooves and a significant amount of white wear debris are the main features on the worn surfaces of the alloy at the temperature from 20 to 600 °C, which are the primary characteristics of severe abrasion wear. Meanwhile, inspection of the composition of white wear debris by the EDS spectrum indicates that the constituents of this debris are the oxides of titanium and aluminum. In addition, there are some distinctions between the worn surfaces produced by different counterface materials. In other words, unlike sliding against Si_3N_4 between 20 and 600 °C, the interaction of the alloy with the Al_2O_3 and SiC leads to tiny grooves, scarce wear debris and smooth worn surfaces, suggesting the alleviation of abrasion wear. This phenomenon is particularly evident at 200 °C, where the worn surface of the alloy against Si_3N_4 is covered by substantial fine oxide particles. When the wear tests are performed at 800 °C, the characteristic features on the worn surfaces of TiAl alloy against Al_2O_3 and SiC are nearly identical to those against Si_3N_4, showing plastic smearing and local tribolayer.

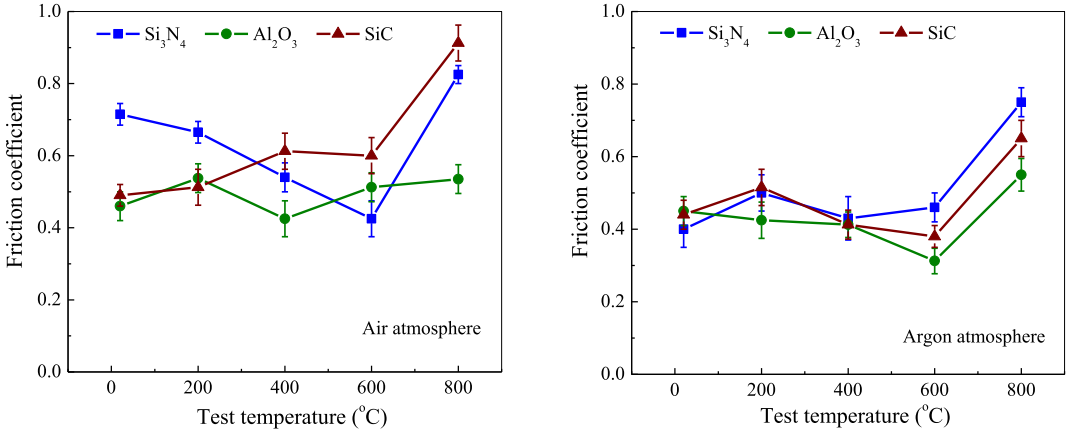

Fig. 3. The friction coefficient of the alloy sliding against Si_3N_4, Al_2O_3 and SiC at different temperatures in air and argon.

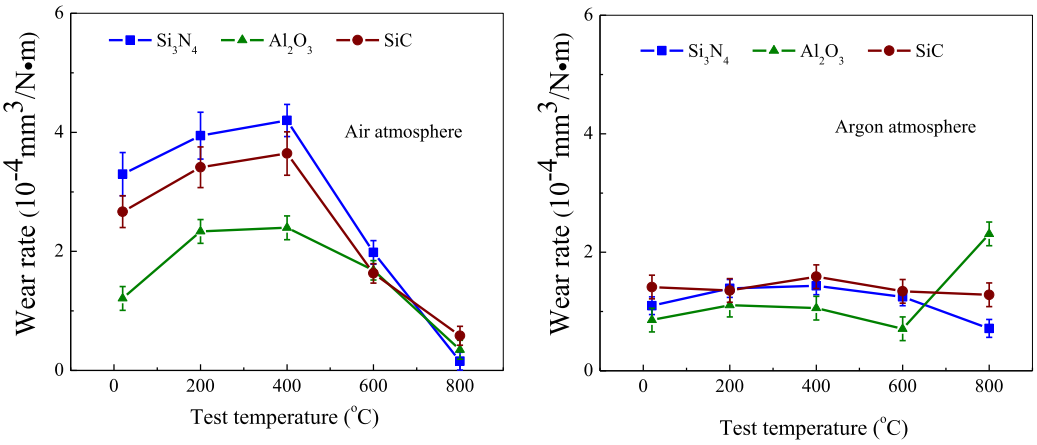

Fig. 4. The wear rate of the alloy sliding against Si_3N_4, Al_2O_3 and SiC at different temperatures in air and argon.

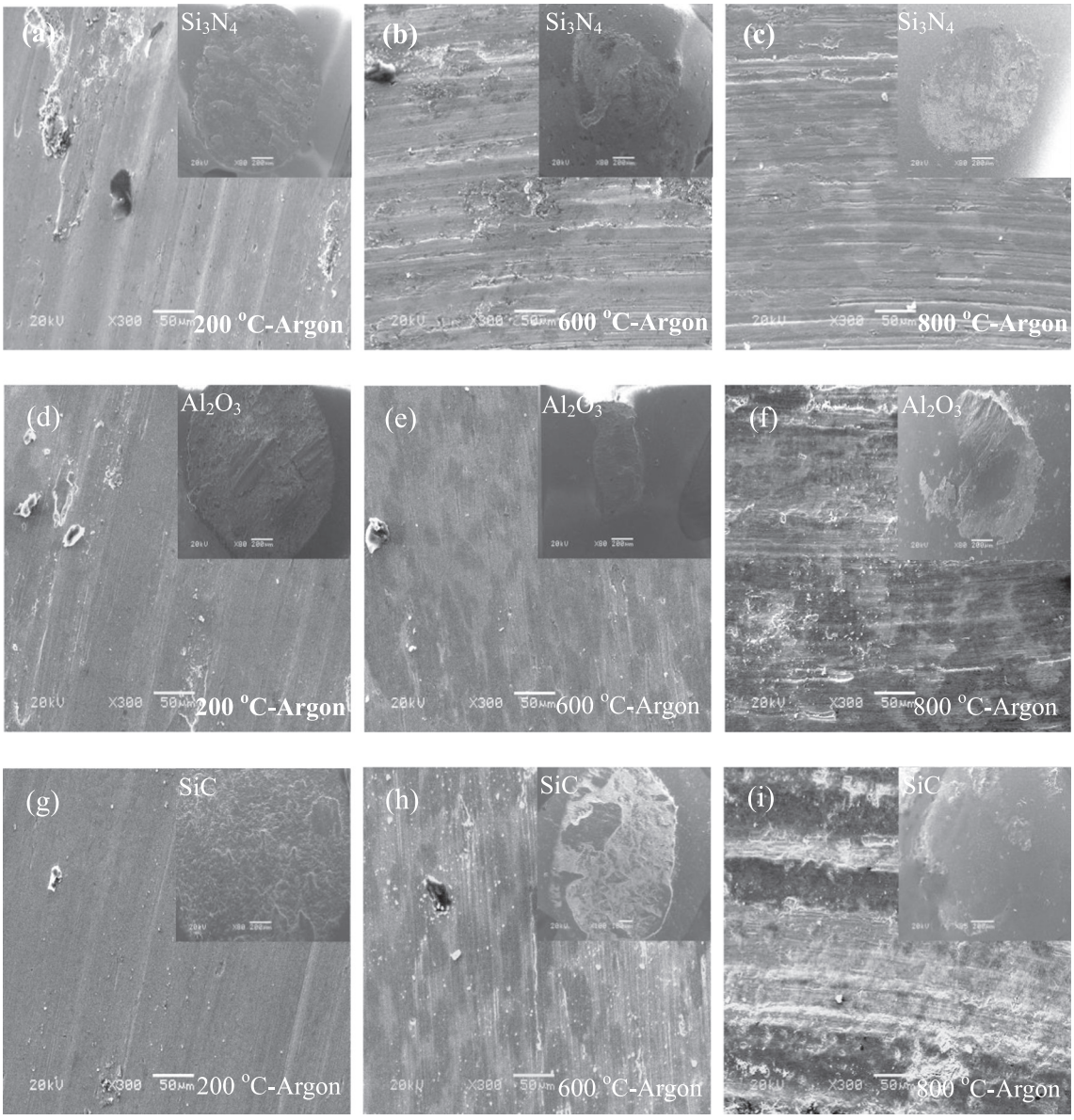

Fig. 5. The SEM images showing the morphologies of the worn surfaces of the alloy and counterface balls at different temperatures in argon.

Table 3
Average element composition (wt. %) of the worn surfaces of counterface balls in argon at different temperature.

Temperature (°C)	Si_3N_4	Al_2O_3	SiC
400	$Si_{9.79}N_{53.57}Al_{23.34}Ti_{11.27}Cr_{0.47}Nb_{1.57}$	$O_{52.31}Al_{33.91}Ti_{8.83}Nb_{4.96}$	$Si_{32.94}C_{17.8}Al_{13.42}Ti_{32.64}Cr_{1.3}Nb_{1.9}$
600	$Si_{2.96}N_{35.81}Al_{24.07}Ti_{28.87}Cr_{1.22}Nb_{7.06}$	$O_{74.55}Al_{21.66}Ti_{1.67}Nb_{2.71}$	$Si_{27.33}C_{11.95}Al_{13.28}Ti_{37.12}Cr_{1.44}Nb_3$
800	Si_{100}	$O_{59.12}Al_{21.1}Ti_{16.68}Cr_{0.60}Nb_{2.5}$	$Si_{60.51}C_{36.92}Al_{0.71}Si_{55.72}Ti_{1.85}$

In an effect to confirm the role of the counterface materials on the wear behavior of TiAl alloy, the surface morphologies of the counterface balls is inserted in Fig. 7 and the surface EDS analysis is provided in Table. 4. In contrast to Si_3N_4 ball, large quantities of debris-transferred layer exist on the worn surface of Al_2O_3 and SiC balls at temperature below 400 °C. EDS analysis also confirms that Ti fraction (indicating the quantity of transfer material to some extent) on the Al_2O_3 and SiC balls are higher than that on the Si_3N_4 ball at this temperature range. With increasing the temperature to 600 and 800 °C, the surface morphologies of the three counterface balls are similar, along with the same amount of transfer material.

Fig. 8 shows the 3D images and cross-section profiles of the worn surfaces of the alloy against different balls at different temperatures in air. Sharper, deeper abrasive grooves and more abundant, fine oxide particles are formed in air than in argon below 600 °C, validated by the 3D images and cross-section profiles. Moreover, at temperature range 20–400 °C the wear scar assigned to the alloy mated with Si_3N_4 ball is much narrower and deeper than that mated with SiC and Al_2O_3 balls, while at 600 °C and 800 °C the cross-section area of the wear scar of the TiAl alloy produced by the three counterface balls are nearly identical and thus their wear rates are analogous.

4. Discussion

4.1. The role of oxidation on the tribological properties of TiAl alloy

On the basis of tribological data and surface analysis, it is inferred that the friction and wear behaviors of the TiAl alloy are strongly related to its surface oxidation and wear debris generated during wear test. As mentioned previously, the friction coefficient of the TiAl alloy is lower in argon than in air from 20 up to 600 °C. This friction behavior may be originating from two factors. First, the fragmented oxide particles acting

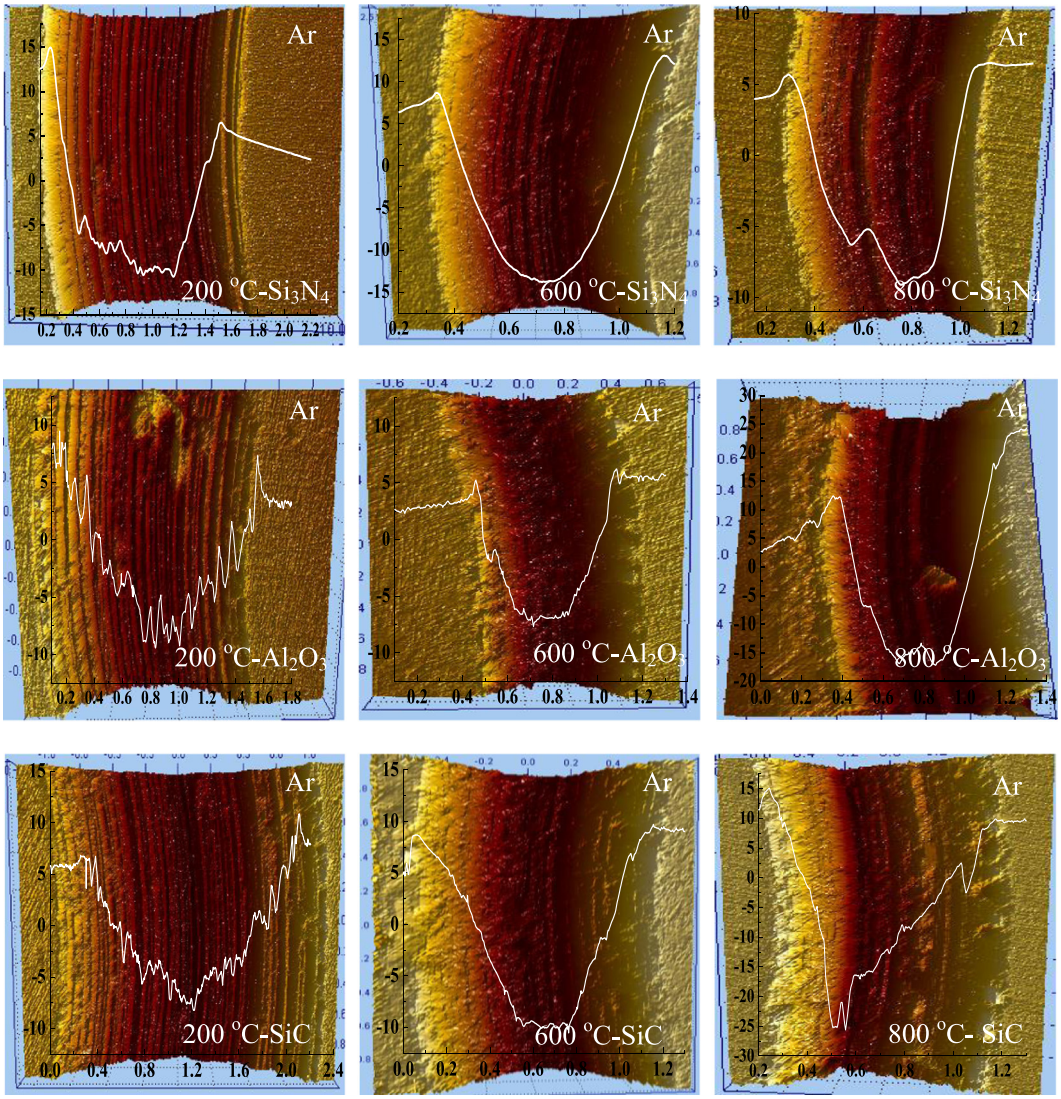

Fig. 6. The 3D images and cross-section profiles of the worn surfaces of the alloy against different balls at different temperatures in argon.

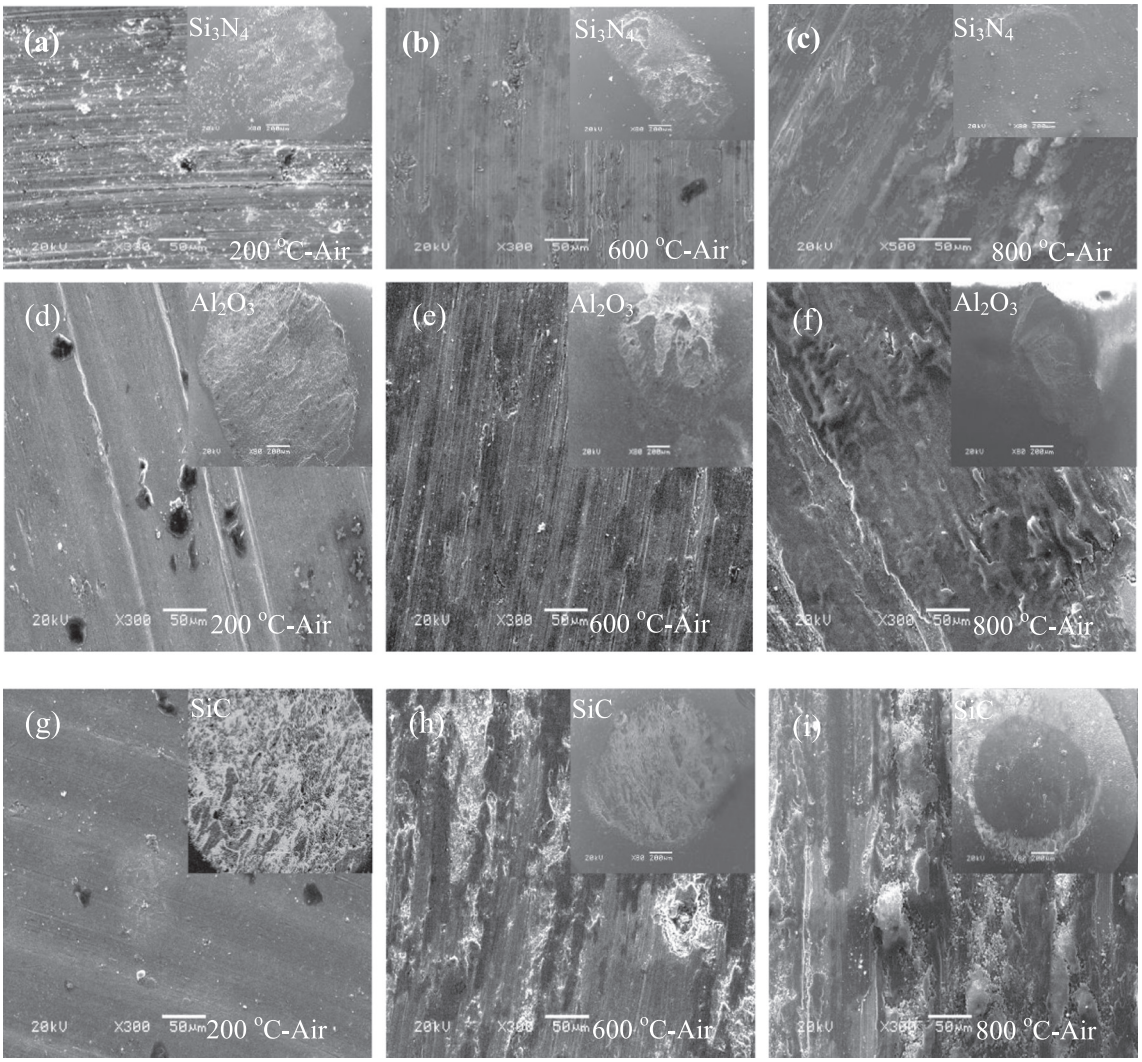

Fig. 7. The SEM images showing the morphologies of the worn surfaces of the alloy and different balls at different temperatures in air.

as cutting tool that will be mentioned below, are contributing to the high friction coefficient in air. Second, at this temperature range in argon, oxidation preferentially takes place for titanium element, providing the lubricity and thus reducing the friction coefficient. However, at 800 °C, Al_2O_3 is predominant on the surface and responsible for the high friction coefficient. The X-ray photoelectron studies on the surface of TiAl alloys by preceding researchers [22,23] confirmed that at low oxygen partial pressure titanium oxidation preceded aluminum oxidation below 600 °C, whereas at higher temperature a much thinner oxide layer consisted predominantly of Al_2O_3. From a thermodynamic point of view, an Ellingham diagram (Fig. 9) has been provided to check the relative thermodynamic stability of Ti- and Al-oxides as a function of temperature and of oxygen partial pressure. It is seen that both the oxidation of Ti and Al is feasible under the experimental oxygen partial pressure (10^{-6} atm). Further, the oxygen equilibrium pressures of Al/Al_2O_3 and Ti/TiO are very similar. Whether $A1_2O_3$ or TiO is stable in equilibrium with the metal phase of Ti–A1 alloys depends on the activities of the metals and the oxides [24]. From the variation of the thermodynamic activities of titanium and aluminum in the region of γ-TiAl, the preferably formed oxide changes from TiO to Al_2O_3 [25]. For 100 °C < T < 600 °C, titanium oxides were reported with Ti in the II, III and IV oxidation states [26–28]. In addition, the amount of Ti(II) species decreases and Ti(IV) species increases, respectively, with increasing temperature [23]. The above analysis confirms the speculations on the preferential oxidation of Ti under low oxygen partial pressures below 600 °C. At higher temperature, i.e. 800 °C, TiO and Ti_2O_3 are oxidized rapidly to TiO_2, whereas the Ti/TiO_2 equilibrium pressure is several orders of magnitude higher than that of Al/Al_2O_3. In this case, TiO_2 could be reduced by aluminum. Therefore, Al_2O_3 is predominant on the surface at 800 °C.

Table 4
The weight concentration (wt. %) of Ti element on the worn surfaces of counterface balls in air at different temperatures.

Temperature (°C)	Si_3N_4	Al_2O_3	SiC
200	1.57	4.86	8.75
600	15.01	18.16	24.67
800	1.6	1.43	1.89

In terms of comparing the worn surfaces in air and argon, it is seen that the worn surfaces produced in argon at the temperature from 20 to 600 °C are relatively smooth and grooves are large and shallow (particularly at low temperature), along with fewer fine particles. In air, much narrower and sharper abrasive grooves are formed. This could mean that the grooves formed in argon are due to the direct contact of the alloy surface with the counterbody surface (with no interposed debris), while in air, the oxidized debris particles are interposed and act as a cutting tool. With further increasing the temperature to 800 °C in argon, the formation of oxide is slight and plowing is still the dominant wear mechanism, which is significantly different from plastic smearing and oxide tribolayer in air. Therefore, how oxidation influences the

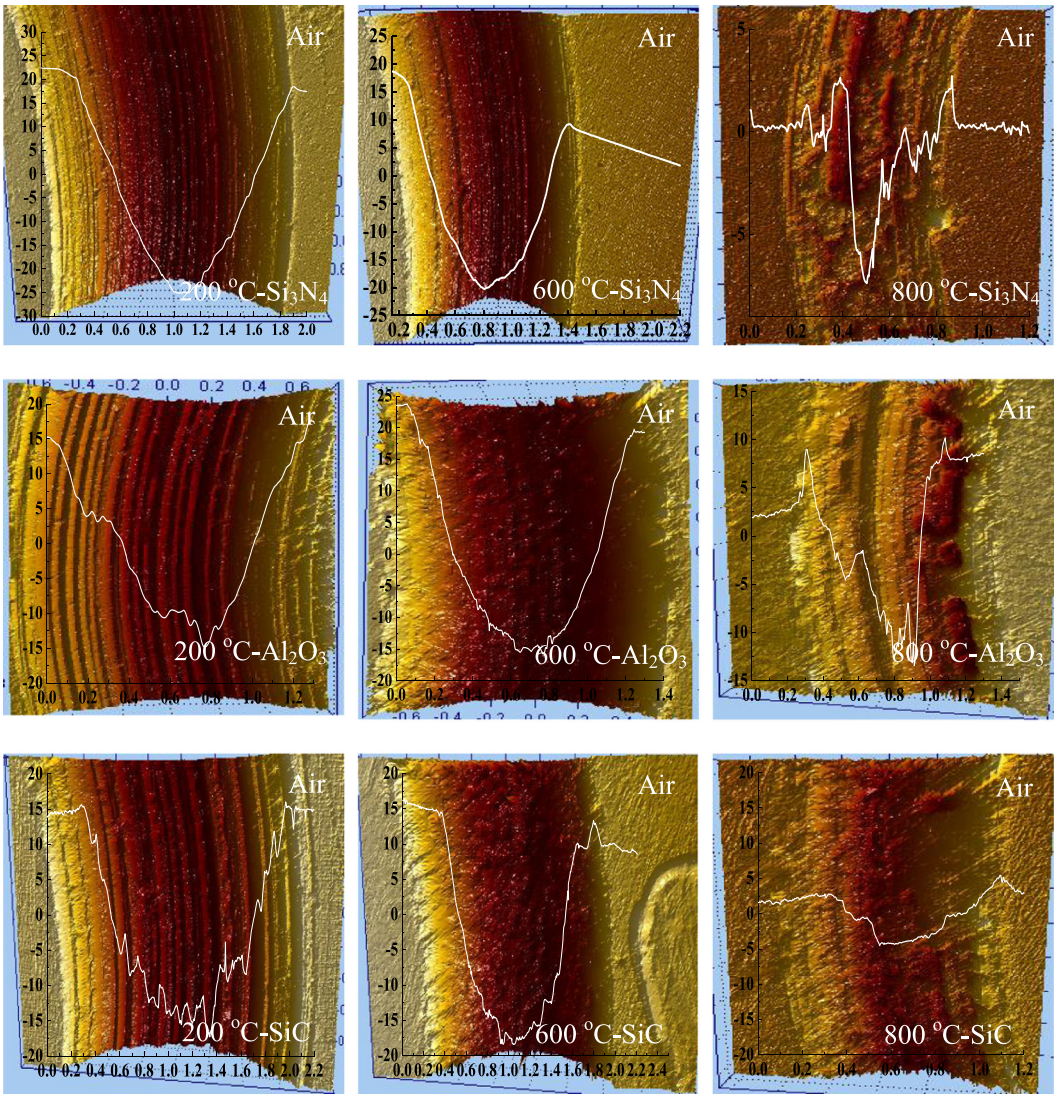

Fig. 8. The 3D images and cross-section profiles of the worn surfaces of the alloy against different balls at different temperatures in air.

wear mechanism is clarified and can be divided into two aspects. A schematic simulating the process is proposed in Fig. 10. From room temperature to 600 °C (Fig. 10a), surface oxidation is relatively low and the alloy does not experience brittle-to-ductile transition. The brittle and hard oxide breaks down into smaller and loose particles under external stress, which reside and tumble in the wear track between the two contact surfaces. These fine oxide particles act as cutting tool, changing the wear mechanism to third-body abrasion and thus, accelerating wear and increasing the friction coefficient. Therefore, surface oxidation is detrimental to the wear-resistant properties of the alloy below 600 °C, and would also be the intrinsic reason for the low wear resistance in air. However, high temperature above 600 °C improves the oxidation rate and enhances sinterability of wear debris. Meanwhile, it is known that TiAl intermetallics experience a brittle-to-ductile transition (BDT) in intervening temperature range, which usually ranges from 600 to 820 °C [29]. In this situation, the good plasticity of the alloy provides the good adherence to the oxidized particles. According to the above two cases, much larger and harder oxide layer is retained on the worn surface and the loose particles fractured by wear stress are sintered together to form compacted layer, performing a protective role on the worn surface in air (Fig. 10b) [30]. In contrast, no oxide layer is found in argon at 800 °C and thus, the wear rate is higher than in air. It is noted that the tribometer sealing system cannot ensure a completely oxygen-free environment, which brings about slight oxidation. As a result, there are some fine particles interposed in the wear track in argon at 800 °C, but severe wear like in air below 600 °C does not occur in such situation.

4.2. Effect of counterface materials on the tribological properties of TiAl alloy

It is found that counterface (Si_3N_4, SiC and Al_2O_3) is an important factor that largely affects the tribological properties of TiAl alloys, and this effect is strongly dependent on the system environment. In air between 20 and 400 °C, the wear rate of TiAl alloy against Al_2O_3 and SiC balls is lower than that with Si_3N_4 as mating surface. Two factors cause this difference in wear rate. First, the debris-transferred layer on the worn surface of Al_2O_3 and SiC balls decreases the direct contact of hard asperities between tribo-pairs to reduce abrasion wear. Second, the fracture toughness of ball counterbodies would be another factor. Si_3N_4 exhibits the highest fracture toughness among the three counterface materials (Table 2). Thus, the asperities on the Si_3N_4 ball are not easily fractured in wear, giving rise to narrow and deeper grooves on the worn surfaces of the alloy and thus assisting wear. At 600 and 800 °C, counterface materials inflict little influence on the wear rate of the TiAl

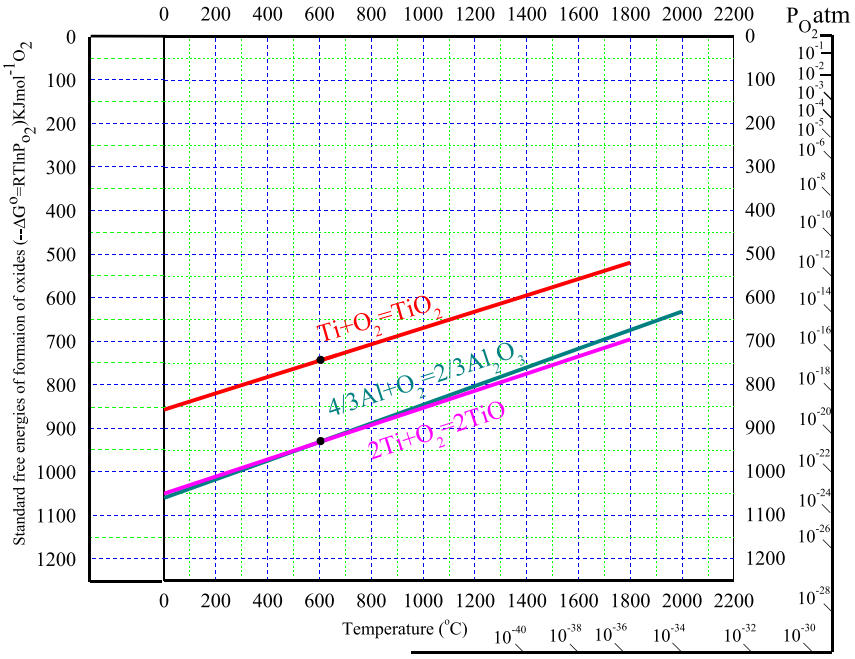

Fig. 9. An Ellingham diagram to check the relative thermodynamic stability of Ti- and Al-oxides as a function of temperature and of oxygen partial pressure.

alloy in air. After analysis, it is found that similar to Al_2O_3 and SiC, the surface of Si_3N_4 ball at 600 °C is covered by considerable amount of transfer materials due to the increased ductility of TiAl alloy. As mentioned above, this transfer material is beneficial to reduce wear in air and therefore the wear rate at 600 °C of the alloy is irrelevant to the ball counterbodies. At 800 °C there is no transfer material seen on the surfaces of all the ball counterbodies (Table. 4) but the wear rates of the alloy against three ball counterbodies are low and close. This may be attributed to the good adherence of the surface to oxides at 800 °C and the formation of protective oxide layer.

When sliding wear is performed at 20 to 600 °C in argon, the worn surfaces present shallow grooves and a small amount of fine oxidized worn debris. This may happen because in argon below 600 °C, oxidation is suppressed to a larger degree and the interface is relatively clean. In this situation, the adhesion force between the contact surfaces is stronger in argon than in air and thus, the wear difference of the TiAl alloy caused by counterface materials in argon is influenced by the adhesion wear. In combination with surface morphologies and composition analysis of the counterface balls, TiAl alloy is more easily transferred to the SiC and Si_3N_4 balls than to the Al_2O_3 ball in the temperature range 20–600 °C, resulting in the slightly higher wear rate. Under high temperature in argon, i.e. at 800 °C, abundant transfer material covers the worn surfaces of Al_2O_3 ball, giving rise to high wear rate of TiAl alloy.

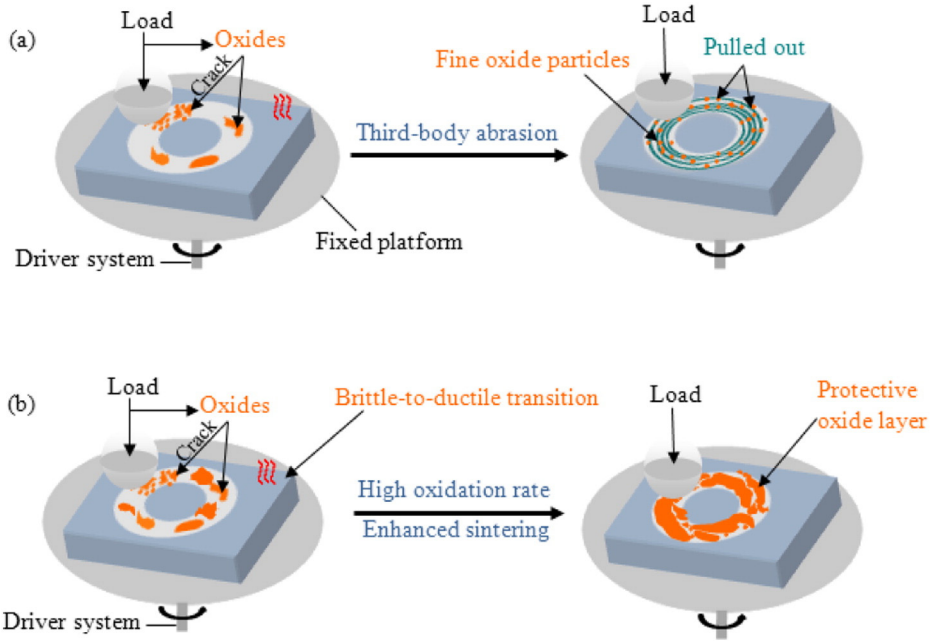

Fig. 10. The schematic simulating the wear process: (a) below 600 °C; (b) above 600 °C.

5. Conclusions

The role of oxidation and counterface materials on the high temperature tribological behaviors of TiAl alloys is clearly shown in this paper. The main conclusions can be summarized as follows:

1. The friction coefficient of the alloy is lower in argon than in air. There is a transition point of the wear rate, i.e. below 600 °C the alloy wears much more in air than in argon but the result is opposite at 800 °C.
2. It is revealed that oxide debris generated at low temperature in air acts as a cutting tool, accelerating wear of the alloy. But above 600 °C in air, high oxidation rate and sinterability, in combined with the increased ductility of TiAl alloy benefit the formation of a protective oxide layer, resulting in improvement of wear resistance.
3. The wear rate of the alloy against Al_2O_3 is lower than that against SiC and Si_3N_4 in argon and air at temperature from 20 to 600 °C, but it is higher at 800 °C in argon.
4. The effect of counterface materials on the wear is strongly dependent on the atmosphere and temperature. In air a significant role of counterface materials on the wear is found below 400 °C but this role is negligible above 600 °C. In argon the difference in the wear rate caused by counterface selection is moderate but pronounced at 800 °C.

Acknowledgments

This work was supported by the National Natural Science Foundation of China (51275507 and 51202258) and the National Basic Research Program of China (2013CB632300).

References

[1] H. Clemens, S. Mayer, Design, processing, microstructure, properties, and applications of advanced intermetallic TiAl alloys, Adv. Eng. Mater. 15 (2013) 191–215.
[2] G. Das, H. Kestler, H. Clemens, P. Bartolotta, Sheet gamma TiAl: status and opportunities, JOM 56 (2004) 42–45.
[3] T. Tetsui, S. Ono, Endurance and composition and microstructure effects on endurance of TiAl used in turbochargers, Intermetallics 7 (1999) 689–697.
[4] G. Das, P.A. Bartolotta, H. Kestler, H. Clemens, in: Y.W. Kim, H. Clemens, A.H. Rosenberger (Eds.),Gamma titanium aluminides 2003, p. PA2003.
[5] X.L. Shi, J. Yao, Z.S. Xu, W.Z. Zhai, S.Y. Song, M. Wang, et al., Tribological performance of TiAl matrix self-lubricating composites containing Ag, Ti_3SiC_2 and BaF_2/CaF_2 tested from room temperature to 600 degrees C, Mater. Des. 53 (2014) 620–633.
[6] D.L. Sun, T. Sun, Q. Wang, X.L. Han, L.L. Guo, Friction and wear properties of TiAl and Ti_2AlN/TiAl composites at high temperature, J. Wuhan Univ. Technol. 28 (2013) 1023–1028.
[7] X.L. Shi, Z.S. Xu, M. Wang, W.Z. Zhai, J. Yao, S.Y. Song, et al., Tribological behavior of TiAl matrix self-lubricating composites containing silver from 25 to 800 degrees C, Wear 303 (2013) 486–494.
[8] J. Cheng, Y. Yu, L.C. Fu, F. Li, Z.H. Qiao, J.S. Li, et al., Effect of TiB_2 on dry-sliding tribological properties of TiAl intermetallics, Tribol. Int. 62 (2013) 91–99.
[9] T. Sun, Q. Wang, D. Sun, G. Wu, Y. Na, Study on dry sliding friction and wear properties of Ti_2AlN/TiAl composite, Wear 268 (2010) 693–699.
[10] J. Cheng, J. Ma, Y. Yu, L. Fu, Z. Qiao, J. Yang, et al., Vacuum tribological properties of a Ti–46Al–2Cr–2Nb intermetallics, J. Tribol. Trans. ASME 136 (2014) 021604.
[11] S.W. Kim, J.K. Hong, Y.S. Na, J.T. Yeom, S.E. Kim, Development of TiAl alloys with excellent mechanical properties and oxidation resistance, Mater. Des. 54 (2014) 814–819.
[12] J. Cheng, F. Li, L. Fu, Z.H. Qiao, J. Yang, W. Liu, Dry-sliding tribological properties of TiAl/Ti_2AlC composites, Tribol. Lett. 53 (2014) 457–467.
[13] H.S. Hong, The role of atmospheres and lubricants in the oxidational wear of metals, Tribol. Int. 35 (2002) 725–729.
[14] Y.C. Liu, J.M. Schissler, T.G. Mathia, The influence of surface oxidation on the wear resistance of cast iron, Tribol. Int. 28 (1995) 433–438.
[15] I. Radu, D.Y. Li, Investigation of the role of oxide scale on Stellite 21 modified with yttrium in resisting wear at elevated temperatures, Wear 259 (2005) 453–458.
[16] S. Wang, J. Ma, S. Zhu, J. Cheng, Z. Qiao, J. Yang, et al., High temperature tribological properties of Ti_3AlC_2 ceramic against SiC under different atmospheres, Mater. Des. 67 (2015) 188–196.
[17] J. Cheng, B. Yin, Z. Qiao, J. Yang, W. Liu, Mechanical and dry-sliding tribological properties of Fe_3Al based composites reinforced by novel $W_{0.5}Al_{0.5}C_{0.5}$ particulates, Mater. Des. 66 (Part A) (2015) 67–76.
[18] J. Qiu, Y. Liu, F. Meng, I. Baker, P.R. Munroe, Effects of environment on dry sliding wear of powder metallurgical Ti–47Al–2Cr–2Nb–0.2 W, Intermetallics 53 (2014) 10–19.
[19] J. Cheng, J. Yang, X. Zhang, H. Zhong, J. Ma, F. Li, et al., High temperature tribological behavior of a Ti–46Al–2Cr–2Nb intermetallics, Intermetallics 31 (2012) 121–126.
[20] C. Li, J. Xia, H. Dong, Sliding wear of TiAl intermetallics against steel and ceramics of Al_2O_3, Si_3N_4 and WC/Co, Wear 261 (2006) 693–701.
[21] Z. Xu, X. Shi, W. Zhai, J. Yao, S. Song, Q. Zhang, Preparation and tribological properties of TiAl matrix composites reinforced by multilayer graphene, Carbon 67 (2014) 168–177.
[22] M.R. Shanabarger, Comparative study of the initial oxidation behavior of a series of titanium–aluminum alloys, Appl. Surf. Sci. 134 (1998) 179–186.
[23] M. Schmiedgen, P. Graat, B. Baretzky, E. Mittemeijer, The initial stages of oxidation of γ-TiAl: an X-ray photoelectron study, Thin Solid Films 415 (2002) 114–122.
[24] A. Rahmel, M. Schütze, W.J. Quadakkers, Fundamentals of TiAl oxidation—a critical review, Mater. Corros. 46 (1995) 271–285.
[25] A. Rahmel, P.J. Spencer, Thermodynamic aspects of TiAl and $TiSi_2$ oxidation: the Al–Ti–O and Si–Ti–O phase diagrams, Oxid. Met. 35 (1991) 53–68.
[26] K. Kovács, I.V. Perczel, V.K. Josepovits, G. Kiss, F. Réti, P. Deák, In situ surface analytical investigation of the thermal oxidation of Ti–Al intermetallics up to 1000 °C, Appl. Surf. Sci. 200 (2002) 185–195.
[27] T.N. Taylor, M.T. Paffett, Oxide properties of a γ-TiAl: a surface science study, Mater. Sci. Eng. A 153 (1992) 584–590.
[28] V. Maurice, G. Despert, S. Zanna, P. Josso, M.-P. Bacos, P. Marcus, XPS study of the initial stages of oxidation of α_2-Ti_3Al and γ-TiAl intermetallic alloys, Acta Mater. 55 (2007) 3315–3325.
[29] Y. Wang, D. Lin, C.C. Law, Brittle-to-ductile transition temperature and its strain rate sensitivity in a two-phase titanium aluminide with near lamellar microstructure, J. Mater. Sci. 34 (1999) 3155–3159.
[30] A. Pauschitz, M. Roy, F. Franek, Mechanisms of sliding wear of metals and alloys at elevated temperatures, Tribol. Int. 41 (2008) 584–602.